N65-31055

PITCH ANGLE DISTRIBUTION AND MIRROR POINT

DENSITIES IN THE OUTER RADIATION ZONE

T. A. Farley[*] and N. L. Sanders

March 1962

Space Technology Laboratories, Inc.

Redondo Beach, California

[*]
Present Address: Institute of Geophysics and Planetary
Physics, University of California at Los Angeles, California.

ABSTRACT

$3/055$

A method is presented for the calculation of the equatorial pitch angle
distribution (unidirectional intensity distribution) of trapped radiation
from the count rate of an omnidirectional detector along a line of force.
An expression is derived for the calculation of the mirror point density
from the equatorial pitch angle distribution. The method is applied to data
obtained from the Space Technology Laboratories scintillation counter and
the University of Chicago proportional counter on the Explorer VI satellive.
The results from the scintillation counter show a relative absence of
electrons with pitch angles of 90° during quiet periods, a sharp increase
in such particles shortly after a sudden commencement magnetic storm, and
restoration of the pre-storm distribution at a higher intensity level after
the storm. The results from the proportional counter are qualitatively
similar with the exception of the apparent deficiency of 90° pitch angles
during quiet periods, which does not appear.

INTRODUCTION

The determination of the spatial distribution of the electrons trapped in the geomagnetic field requires a great many samplings of the particle intensity at different locations throughout the field. The Explorer VI satellite, with a period of 12 hours and 42 minutes, crossed the line of force at an equatorial geocentric radius of 21,000 km either two or four times per period. Sufficient data was obtained from these crossings during a three week period to permit detailed analysis of the spatial distribution along this line in terms of the individual particle orbits. The observations covered a range of geomagnetic latitudes from 0° to 50°.

This satellite was launched on August 7, 1959 into an elliptical orbit with apogee at 48,600 km from earth center. A scintillation counter, one of three radiation experiments on board, was supplied by Space Technology Laboratories, Inc. Rosen and Farley (1961) have given a detailed description of this instrument and the data obtained from it. All count rates of this instrument used in this paper have been corrected for saturation effects as described by Rosen and Farley. The efficiency of the instrument for detection of electrons is given in Figure 1.

A proportional counter was supplied by the University of Chicago for this satellite and detailed results from that instrument have been given by Fan, et al. (1961). Some of the count rate data published by Fan, et al. have been used here for the calculation of pitch angle distributions.

The problem of calculating unidirectional intensities at a point from knowledge of the omnidirectional intensity at every point along a line of force has been solved by Ray (1960). The form of the solution presented by him differs from that presented in this paper. Approximate solutions to

this same problem have been obtained by Fan, et al. (1961) and by Wentworth (1962), both of whom apply their solutions to the data obtained from the proportional counter on Explorer VI.

Exact expressions for the equatorial unidirectional intensity (pitch angle distribution) and the mirror point density are presented in this paper in a simple form. These theoretical results are then applied to the omnidirectional intensities measured by the scintillation counter and proportional counter on the Explorer VI satellite. The unidirectional intensities calculated from the exact expressions derived herein are in excellent agreement with those calculated from the same data by the approximation technique of Wentworth. Comparison is made between the pitch angle distributions calculated from the data and that calculated from the omnidirectional intensities given by Hess and Killeen (1961) for neutron-decay electrons.

THEORETICAL DISCUSSION

The equilibrium distribution of trapped particles obeying the adiabatic invariance conditions along any line of force may be described in at least three different ways: by the omnidirectional particle intensity at all points along the line, by the unidirectional intensity at all pitch angles at the geomagnetic equator, and by the density of particles having mirror points at each point along the line. In a given magnetic field these three descriptions are equivalent, contain exactly the same information, and are convertible one to another. The equatorial pitch angle distribution is derived here from the omnidirectional intensity along the line of force for an arbitrary magnetic field. The mirror point density is derived here from the equatorial pitch

angle distribution by assuming that the field is a magnetic dipole.

Definitions

The pitch angle α is the angle between the particle velocity vector and the magnetic field vector at the point where the magnetic field magnitude is B. It is equal to 90° at the particle mirror point and has a minimum value when the particle crosses the equator.

The unidirectional intensity j (B, cos α) is the number of particles per cm^2 per sec ster having velocity vectors between α and $\alpha + d\alpha$.

The omnidirectional intensity J(B) is the integral of j (B, cos α) over the solid angle. B_o, j_o, etc. refer to the values of the variables at the geomagnetic equator. B_m refers to the value of the magnetic field at the particle mirror point.

j_o (cos α_o), the unidirectional intensity in the equatorial plane, is called the pitch angle distribution.

The mirror point density $\omega(\lambda)$ is the number of particles per unit volume having mirror points between the geomagnetic latitudes λ and $\lambda + d\lambda$.

$T(\lambda)$ is twice the time required for a particle to travel from its northern mirror point at λ to its southern mirror point at $-\lambda$, i.e., one complete period.

Pitch Angle Distribution

From the definition,

$$J(B) = 4\pi \int_{\alpha_{min}}^{\pi/2} j(B, \cos \alpha) \sin \alpha \, d\alpha \qquad (1)$$

$j_o(\cos \alpha_o)$ can be obtained from the solution of this integral equation as follows. Consider a group of particles which have equatorial pitch angles

between α_o and $\alpha_o + d\alpha_o$, and which mirror between λ and $\lambda + d\lambda$. Neglecting their slow longitudinal drift, the guiding centers of these particles move on a bundle of flux lines which constitute a flux tube extending from λ to $-\lambda$. In equilibrium, the same number of guiding centers per unit time must cross one tube section in one direction as cross any other tube section in the same direction. Thus:

$$2\pi j \ (B, \ \cos \alpha) \ \sin \alpha \ d\alpha \ \cos \alpha \ dA = 2\pi j_o \ (\cos \alpha_o) \ \sin \alpha_o \ d\alpha_o \ \cos \alpha_o \ dA_o$$

Using the mirror relation for adiabatically trapped particles,

$$\frac{\sin^2 \alpha_o}{B_o} = \frac{\sin^2 \alpha}{B} \ ,$$

$$j \ (B, \ \cos \alpha) \ BdA \ = \ j_o \ (\cos \alpha_o) \ B_o dA_o$$

and therefore

$$j \ (B, \ \cos \alpha) \ = \ j_o \ (\cos \alpha_o)$$

This equality states that the unidirectional intensity at some α_o at the geomagnetic equator is equal to the unidirectional intensity at α at any point along the line of force if α is related to α_o by the mirror equation. Equation (1) can be rewritten as

$$J(B) \ = \ 4\pi \int_{\alpha_{min}}^{\pi/2} j_o \ (\cos \alpha_o) \ \sin \alpha \ d\alpha \qquad (2)$$

Using the mirror equation $\sin^2 \alpha = \dfrac{B}{B_m}$, the variable of integration may be changed to B_m:

$$\frac{J(B)}{2\pi B} = \int_{B}^{B_{max}} \frac{J_o'(B_m)\ dB_m}{(B_m)^{3/2}\ (B_m - B)^{1/2}} \tag{3}$$

where $J_o'(B_m)$ is the function which is obtained by changing the variable
in J_o from $\cos \alpha_o$ to B_m. B_{max} is the value of the field at which the
particle having pitch angle α_{min} mirrors. Notice that those particles
having mirror points at $B_m < B$ (i.e., higher altitudes) do not contribute
to $J(B)$.

Making the substitutions

$$B_m = B_{max} - y$$

$$B = B_{max} - t$$

$$\frac{J_o'(B_m)}{(B_m)^{3/2}} = \frac{J_o'(B_{max} - y)}{(B_{max} - y)^{3/2}} = f(y)$$

$$\frac{J(B)}{2\pi B} = \frac{J(B_{max} - t)}{2\pi(B_{max} - t)} = \psi(t)$$

equation (3) becomes

$$\psi(t) = \int_{0}^{t} \frac{f(y)\ dy}{(t - y)^{1/2}} \tag{4}$$

with $\psi(0) = 0$ since $J(B_{max}) = 0$.

This is Abel's Integral Equation and its solution is (e.g., Courant, 1956).

$$f(t) = \frac{1}{\pi} \frac{d}{dt} \int_0^t \frac{\psi(y)\ dy}{(t-y)^{1/2}} \qquad (5)$$

Integrating by parts, differentiating under the integral sign, and replacing the original variables:

$$j_o(\cos \alpha_o) = j_o'(B_m) = -\frac{(B_m)^{3/2}}{\pi} \int_{B_m}^{B_{max}} \frac{\frac{d}{dB}\left|\frac{J(B)}{2\pi B}\right| dB}{(B-B_m)^{1/2}} \qquad (6)$$

Equation (6) is the general solution for $j_o(\cos \alpha_o)$ when $J(B)$ is known. The differentiation and integration may be performed by computer. The change of variable from B_m to $\cos \alpha_o$ is accomplished through the mirror relation $\sin^2 \alpha_o = \frac{B_o}{B_m}$.

Mirror Point Density

Those particles which have equatorial pitch angles between α_o and $\alpha_o + d\alpha_o$ have mirror points between λ and $\lambda + d\lambda$. In equilibrium, the time rate at which the guiding centers of these particles pass through the cross section of a flux tube at the equator is equal to the time rate at which they mirror in the volume element $dAdl$ of the flux tube at λ:

$$4\pi j_o (\cos \alpha_o) \sin \alpha_o d\alpha_o \cos \alpha_o\ dA_o = \frac{\omega(\lambda)\ dldA}{T(\lambda)}$$

where ω and T are the mirror point density and bounce period as previously

defined. In cylindrical coordinates $(dl)^2 = dr^2 + r^2(d\lambda)^2$, and for a dipole field

$$dl = r_o \cos^7 \lambda \frac{B}{B_o} d\lambda$$

where r_o is the geocentric radius in the equatorial plane. Therefore

$$\omega(\lambda) = \frac{2\pi T(\lambda)}{r_o \cos^7 \lambda} \left(\frac{B_o}{B}\right)^2 \left(\frac{1}{B_o}\frac{dB}{d\lambda}\right) J_o (\cos \alpha_o) \qquad (7)$$

In a dipole field

$$\frac{B}{B_o} = \frac{(4 - 3 \cos^2 \lambda)^{1/2}}{\cos^6 \lambda} \qquad (8)$$

so that

$$\frac{1}{B_o}\frac{dB}{d\lambda} = 3 \tan \lambda \left[\frac{B_o}{B \cos^{10}\lambda} + \frac{2B}{B_o} \right] \qquad (9)$$

From the definition of the bounce period,

$$T(\lambda) = 4 \int_0^{B_m} \frac{dl}{v \cos \alpha} = \frac{4 r_o}{v} \int_0^\lambda \frac{B}{B_o} \frac{\cos^7\lambda d\lambda}{(1 - \frac{B}{B_m})^{1/2}} \qquad (10)$$

Equation (10) has been numerically integrated, and the results are shown in Fig.2.2. The bounce period is evidently inversely proportional to the particle velocity. The period, often described as approximately independent of the mirror latitude, actually varies by a factor of approximately 1.7 from the geomagnetic equator to a latitude of 60°.

Bringing together equations (7), (8), and (9), the result is

$$\omega(\lambda) = \frac{6\pi T(\lambda) \sin \lambda (8-5 \cos^2\lambda)}{r_0(4 - 3 \cos^2\lambda)^{3/2} \cos^2\lambda} \; j_0'(\lambda) \qquad (11)$$

where $j_0'(\lambda)$ is the result of a change in variable from $\cos \alpha_0$ to λ in $j_0(\cos \alpha_0)$.

If the particles are all of the same velocity (e.g., all relativistic), then equation (8) may be used together with values of T from Fig. 2 to obtain the mirror point density from the pitch angle distribution.

Detector Efficiency

The ideal instrument for measurements of the omnidirectional intensities for use in these expressions is one whose directional response is isotropic and whose energy response is constant within some energy interval and zero elsewhere. Such an instrument would produce data from which a correct pitch angle distribution could be calculated for the particles in that energy interval.

If the detector response is anisotropic in such a way that the efficiency depends on the pitch angle and local satellite orientation, the data are not readily usable to calculate the pitch angle distribution.

If the instrument is omnidirectional, but has an efficiency which depends on energy, the omnidirectional count rate R(B) will be given by

$$R(B) = 4\pi \int_\alpha \int_E \epsilon(E) \; \frac{dj'(B,E, \cos \alpha)}{dE} \; \sin \alpha d\alpha dE$$

If $j'(B,E, \cos \alpha)$ can be written as $j(B, \cos \alpha) n(E)$, which indicates that the energy spectrum does not change along a line of force, then

-9-

$$R(B) = \left[\int_E \epsilon(E) \frac{dn(E)}{dE} dE \right] 4\pi \int_\alpha j(B, \cos \alpha) \sin \alpha d\alpha = kJ(B)$$

and an undistorted pitch angle distribution will result.

If the energy spectrum does change along a line of force (and therefore changes with pitch angle at a given point on the line), the unidirectional intensities determined from the observed count rates will be weighted (distorted) according to the efficiency of the detector for particles from that direction. For example, if the efficiency of the detector rises with energy, the unidirectional intensities will appear too large in the directions from which the high energy particles come, and too low in the directions from which low energy particles come.

Data and Results

The data from which the pitch angle and mirror point distributions have been calculated are the count rates of the scintillation experiment at the time the satellite crosses one particular geomagnetic field line. The field line which crosses the geomagnetic equator at 21,000 km from earth center has been chosen because the satellite crossings of this line take place over a wide range of northern latitudes, and because comparisons with the published results of Fan, et al., can be made along this same line of force. This field line is also the approximate position of one of the outer zone electron peaks observed by the scintillation counter and designated peak 2 by Rosen and Farley (1961). The position of the field line in space has been calculated from an earth-centered dipole approximation in which the north geomagnetic pole intersects the surface of the earth at 78.5°N latitude and 291°E longitude.

The data points have been grouped into three time intervals.
Figure 3 shows the data from all available crossings of this line of force
during the magnetically quiet period from August 8 - August 16, 1959.
Figure 4 shows data points taken during the magnetically disturbed period
of August 18 - August 22, which followed the severe magnetic storm of
August 16, 1959. Figure 5 includes data taken during a quiet period
following the storm. The data points have been divided in this way to
show the major changes which took place during these three weeks.

The assumption has been made that these count rates are proportional
to the omnidirectional particle intensity at the point in space at which
the data was taken. This is equivalent to the assumption that the counter
efficiency ϵ is independent of particle pitch angle for all satellite
orientations. Even though the scintillation counter is averaging over
each spin cycle of the vehicle, its efficiency is still anisotropic in
such a way that it is more sensitive to particles striking the vehicle
parallel to the spin axis direction than to particles striking perpendicular
to the spin axis direction. Near the geomagnetic equator at 21,000 km the
vehicle spin axis was approximately perpendicular to the magnetic field
line so that the instrument was most sensitive to particles having 90°
pitch angles. Therefore the apparent absence of these particles, which is
a result of the decreased count rate near the equator, cannot be explained
by the somewhat anisotropic response of the counter. Except for the apparent
hole near 90° and the loss cone near 0° the pitch angle distribution is nearly
isotropic at the equator, and a somewhat anisotropic response is of little
consequence. At high latitudes, where the pitch angles are all near 90°,

considerable error which depends on the satellite orientation can be introduced. Because of the existing uncertainties in vehicle orientation with respect to the line of force, no attempt has been made to omit data points or to correct for these errors, which certainly contribute to the data point scatter at the high latitudes. Crossings of the line of force at northern latitudes have been plotted with solid circles and those at southern latitudes with open circles. The line drawn through these points represents our best estimate of the omnidirectional particle intensity.

Comparison has been made in each figure with the count rate of the University of Chicago proportional counter rate (Fan, et al., 1961). Since the University of Chicago group used the line of force passing through their E_3 outer zone maximum, their curve in Fig. 3 is for a neighboring line of force at R_o = 23,000 km, while in Figs. 4 and 5 their curve is for the same line as the scintillation counter data. In each case the proportional counter data has been normalized to the scintillation counter rate at the geomagnetic equator, even though the post-storm intensity increase is considerably greater for the scintillation counter than for the proportional counter.

We attribute the change in count rate ratio of these two counters along the line of force to a small change in the average electron energy along the line of force. For example, a small increase in the proportion of high energy electrons (>1 Mev) would cause the observed increase in proportional counter to scintillation counter ratio near the geomagnetic equator because the proportional counter efficiency is proportional to $E^{4.7}$ (Fan et al., 1961) while the scintillation counter efficiency is rising only slowly in this energy range (Fig. 1).

The authors believe that the scintillation counter is responding entirely to electrons of energies above 500 kev because of the improbably large fluxes of electrons below this energy which would be required to cause a significant fraction of the observed counting rate. Therefore, the pitch angle distributions calculated from the scintillation counter data are those for electrons above 500 kev, weighted by the slowly rising efficiency of the counter. The distributions calculated from the proportional counter data are those for the entire electron energy spectrum, weighted by $E^{4.7}$. If there are changes in the energy spectrum along the line of force the scintillation counter distributions will be only mildly distorted while those of the proportional counter may suffer from a very considerable distortion according to the argument presented in the theoretical section.

A number of qualitative similarities between the STL and Chicago data may be pointed out. First, there is a sharp peaking up of the count rate curves of both counters at the geomagnetic equator during the magnetic storm recovery phase. Unfortunately, there are few crossings of this line of force at intermediate latitudes during this period, and the STL count rate curve has simply been drawn in a shape similar to that of the preceding period at these latitudes. Second, there is a return to the pre-storm count rate curve shape during the third, magnetically quiet, period.

Figures 6, 7, and 8 are presentations of the corresponding equatorial pitch angle distributions computed by the method described in the theoretical section. Since the unidirectional intensity has been plotted against the cosine of the pitch angle, the area under each curve is simply the count rate

-13-

of each instrument at the geomagnetic equator. Because of the equatorial normalization of the count rates of the instruments, both the scintillation and proportional counter curves have the same total areas. The equatorial peaking of the count rate curve during the storm is apparent here as a sharp increase in particles having pitch angles near 90°. It does not seem possible to say whether these particles have been removed by August 24, or whether they have been distributed over smaller pitch angles.

The pitch angle distributions given here for the proportional counter differ substantially from those given by Fan, et al., (1961), primarily because of a different definition of the pitch angle distribution used by them.

Figure 9 is a plot of the mirror point distributions which correspond to the three time periods, calculated from the scintillation counter data.

Experimental Discussion

The equatorial pitch angle distributions calculated from the scintillation counter data are compared with a theoretical distribution of neutron-albedo decay electrons in Fig. 10. The theoretical distribution has been computed from the omnidirectional intensity presented by Hess and Killeen (1961) for the neutron-decay electrons along the line of force at r_0 = 20,500 km. All three curves in this figure have been arbitrarily normalized at $\cos \alpha_0$ = 0.66.

The neutron-albedo decay theory is so far the only theoretical source mechanism for the outer zone electrons from which a pitch angle distribution has been calculated, and it is for that reason that these comparisons have been made. The authors believe that the Explorer VI results indicate the presence of substantial fluxes of electrons of energies of at least 1 Mev,

and that the flux of these particles increased markedly after a geomagnetic storm. These facts appear to be incompatible with the existence of an unmodified neutron-decay electron energy spectrum in this region. Indeed, the only part of the neutron-decay hypothesis which is compatible with the observations is the possibility that neutron decay is the source mechanism for electrons which are subsequently modified both in energy and pitch angle distribution by an unknown time-dependent mechanism.

The magnetic history of the period for which data has been presented may be summarized as follows: August 12, 13, and 14 were among the five quietest days in August. On August 15, a gradual commencement storm was reported at some stations. At approximately 0400 on August 16, a sudden commencement storm began which continued until the end of the 17th or beginning of the 18th. This storm was classed as severe (corresponding to a K-index of 8 or 9). Huancayo reported a moderate, gradual commencement storm which began at 0635 on August 18 and ended at 2000 hours the same day. A moderately severe, sudden commencement storm began on August 20 at 0412. There is no general agreement as to when this storm ended. (Some stations estimated that it ended the 20th while others recorded disturbed conditions until August 24). August 27 and 28 were the two quietest days of the month.

During the two magnetically quiet periods, there appears to be a relative absence of particles having pitch angles near 90°. This fact is a consequence of the decreasing count rate near the geomagnetic equator. Mathematically speaking, the intensity of particles having pitch angles of 90° is found by subtracting from the equatorial count rate the contribution of all particles mirroring at higher latitudes, and designating the remainder as the count rate

of particles having 90° pitch angles. If this remainder is small (as is actually the case) it will be quite sensitive to any variation or error in the count rate at the equator. For example, the decrease in count rate at the equator of less than 15% (Figs. 2.3 and 2.5) causes a drop of approximately 100% in the pitch angle distribution at 90° (Figs. 2.6 and 2.8). Nevertheless, the assertion that there is a relative absence of particles with pitch angles near 90° during quiet periods appears justified by the data.

During the magnetic storm main and recovery phases either a sub-stantial number of new particles are injected, or else acceleration of particles already present takes place, causing the twentyfold increase in count rate of the scintillation counter. The injection or acceleration must be such as to increase sharply the intensity of particles trapped near the geomagnetic equator. High latitude injection or acceleration of geo-magnetic storm electrons, therefore, appears inconsistent with the data.

The disappearance of the electrons with pitch angles near 90° takes place sometime after the pass 29 crossing of the line of force at 1232 UT on August 22, 1959 during a period of lessening magnetic disturbance. August 22 is also the date on which a great solar radio noise storm commenced, and the possible connection of this storm with the outer radiation zone has been discussed by Arnoldy, et al., (1960). How this solar event might have influenced electrons with pitch angles near 90° deep within the geomagnetic field is not known. The fact that the resulting pitch angle distribution resembles the pre-storm distribution may indicate that it is the result of the same mechanism which produced the pre-storm distribution at some earlier date.

APPENDIX

A useful analytic solution to Equation (6) can be found if J(B) can be conveniently expressed as a polynomial in B, i.e.,

$$J(B) = \sum_{k=-s}^{k=n} A_k B^k \quad \text{where s and n are positive}$$

integers.

Then

$$2\pi \frac{d\psi}{dB} = \sum_{k=-s}^{k=n} (k-1)A_k B^{k-2}$$

Substituting into Equation (6) and performing the integration we find that

$$4\pi J_o'(B) = \frac{2B^{3/2}}{\pi} \left\{ 2(B_{max}-B)^{1/2} \sum_{k=2}^{k=n} (1-k)B^{k-2} A_k \right.$$

$$\left. + \sum_{i=-s}^{i=0} (1-i) A_i I_i \right\} \tag{12}$$

where

$$I_i = \frac{(B_{max} - B)^{1/2}}{(i-1)B_{max}^{i-1} B} + \frac{1-2i}{2-2i} \left(\frac{1}{B}\right) I_{i+1} , \quad i < 0$$

and

$$I_0 = \frac{(B_{max} - B)^{1/2}}{B\, B_{max}} + \frac{1}{B^{3/2}}\cos^{-1}\left(\frac{B}{B_{max}}\right)^{1/2}$$

For each value of B, $j(\cos\alpha_0)$ is equal to that value of $j'(B)$ for which

$$\cos\alpha_0 = \left(1 - \frac{B_0}{B}\right)^{1/2}$$

In using the above derived expressions, it is usually convenient to express B in units of B_0, the value of the magnetic field intensity in the equatorial plane.

ACKNOWLEDGMENTS

The authors are indebted to Dr. Robert Wentworth for
discussions concerning his technique for determining pitch
angle distributions. Dr. Wilmot Hess and Dr. John Killeen
have kindly provided their calculated flux data and mirror
point density curves for the neutron-albedo electron
population mechanism. Adeline Cowen has spent many hours
in data reduction and calculation.

REFERENCES

Arnoldy, R. L., R. A. Hoffman, and J. R. Winckler, Observations of the Van Allen radiation regions during August and September 1959, Part I, J. Geophys. Research 65 (5), 1361 - 1376, 1960.

Courant, R., Differential and Integral Calculus, Interscience Publishers Inc., New York, (1956) p. 340.

Fan, C. Y., P. Meyer, and J. A. Simpson, The equatorial pitch angle distribution of electrons in the outer radiation belt, IGY Satellite Report No. 14, 15-21, 1961a.

Fan, C. Y., P. Meyer, and J. A. Simpson, Dynamics and structure of the outer radiation belt, J. Geophys. Research 66 (9), 2607-2640, 1961b.

Hess, W. N. and J. Killeen, Spatial distribution of electrons from neutron decay in the outer radiation belt, J. Geophys. Research 66 (11), 3671-3680, 1961.

Ray, E. C., On the theory of protons trapped in the earth's magnetic field, J. Geophys. Research 65 (4), 1125-1134, 1960.

Rosen, A., and T. A. Farley, Characteristics of the Van Allen radiation zones as measured by the scintillation counter on Explorer VI, J. Geophys. Research 66 (7), 2013 - 2028, 1961.

Wentworth, R. C., Conversion matrices between pitch angle distribution and omnidirectional counting rates, J. Geophys. Research, in press.
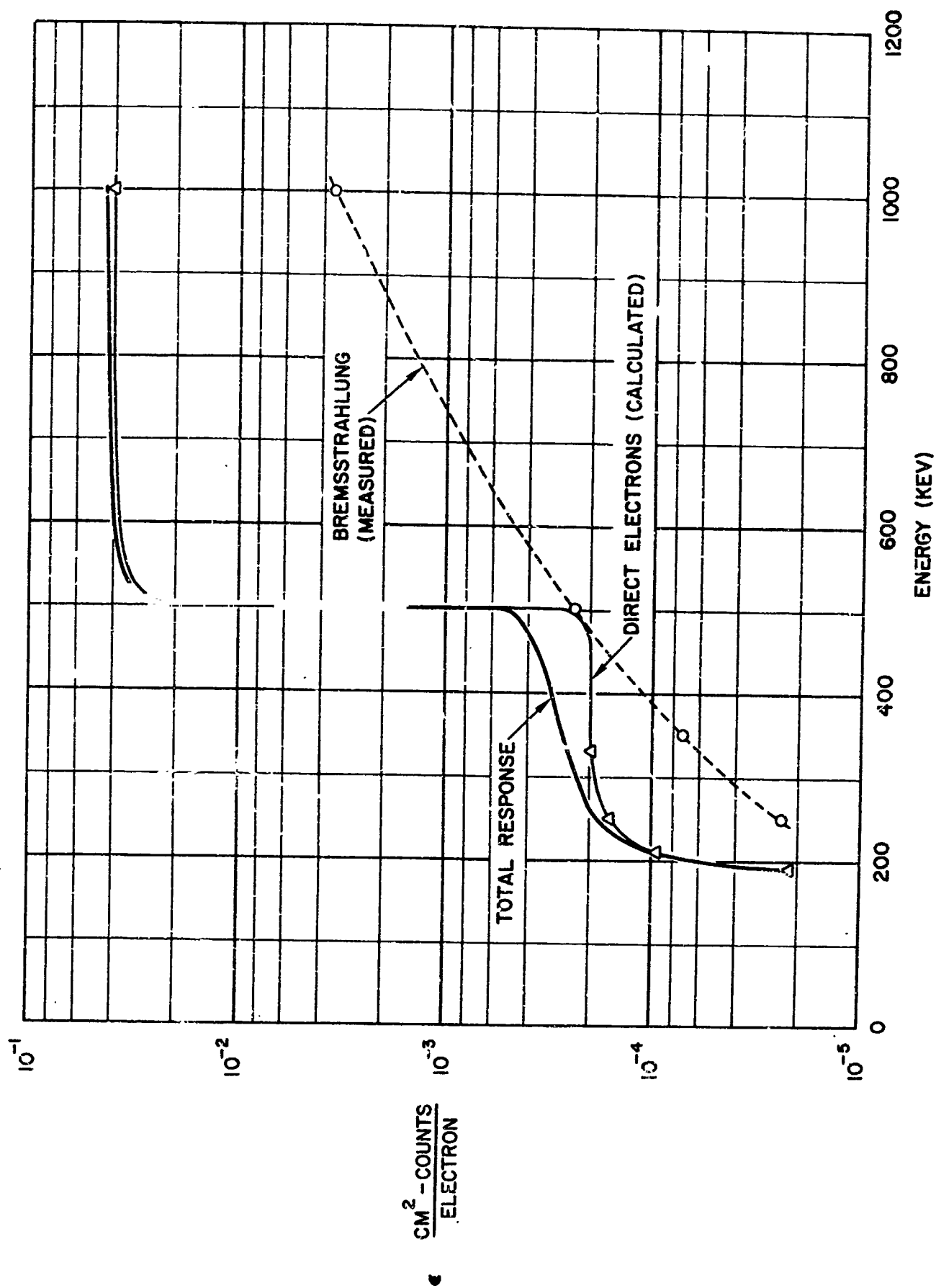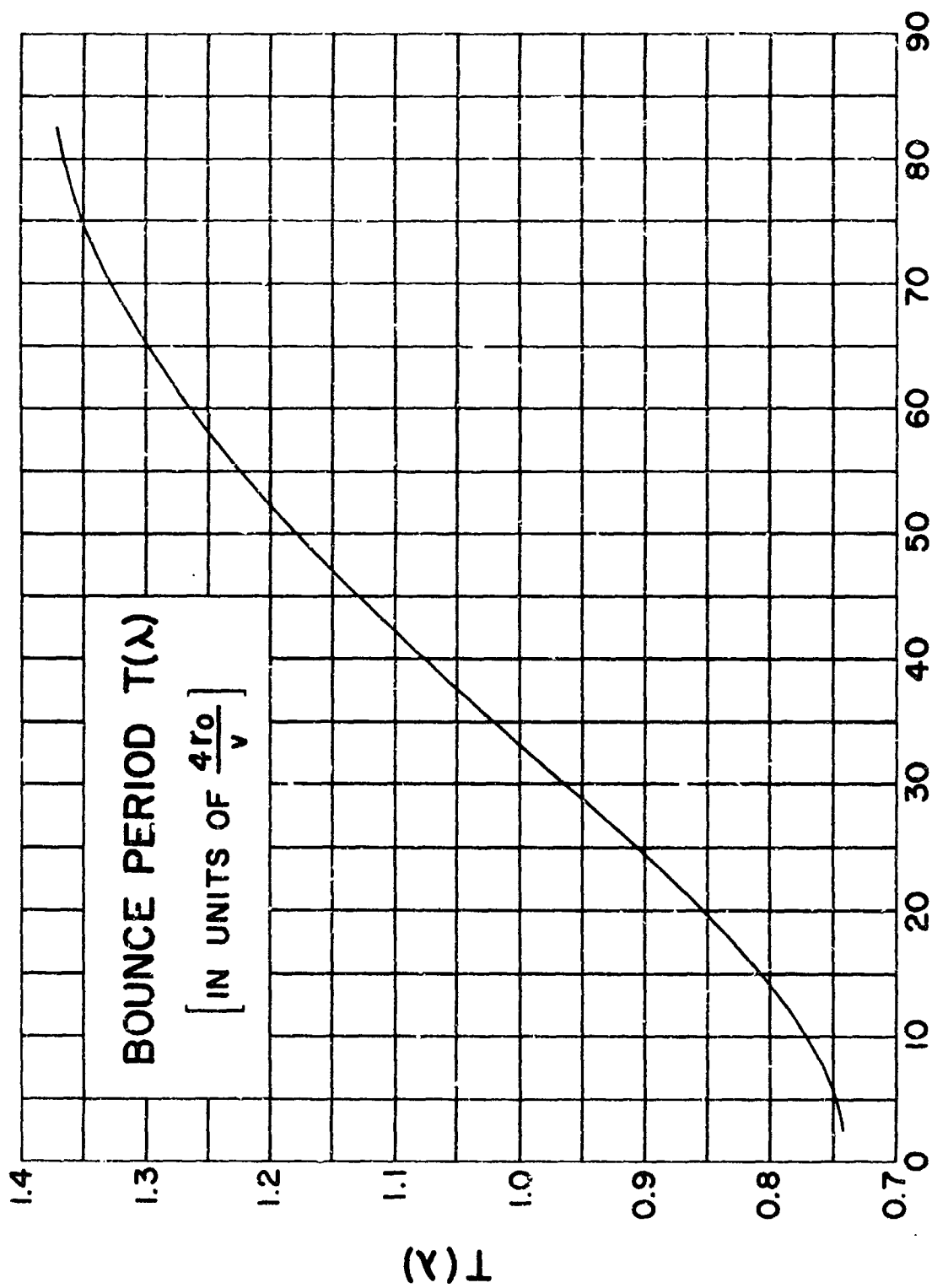
Fig. 1: The efficiency of the scintillation counter for the detection of electrons.

Fig. 2: The bounce period of particles adiabatically trapped in a dipole field plotted as a function of the latitude at which the particle mirrors. r_o is the geocentric radius of the line of force in the equatorial plane, and v is the particle velocity.

AUGUST 8-16

—— SCINTILLATION
COUNTER
$r_o = 21,000$ KM

- - - - PROPORTIONAL
COUNTER
$r_o = 23,000$ KM

GEOMAGNETIC LATITUDE -DEGREES
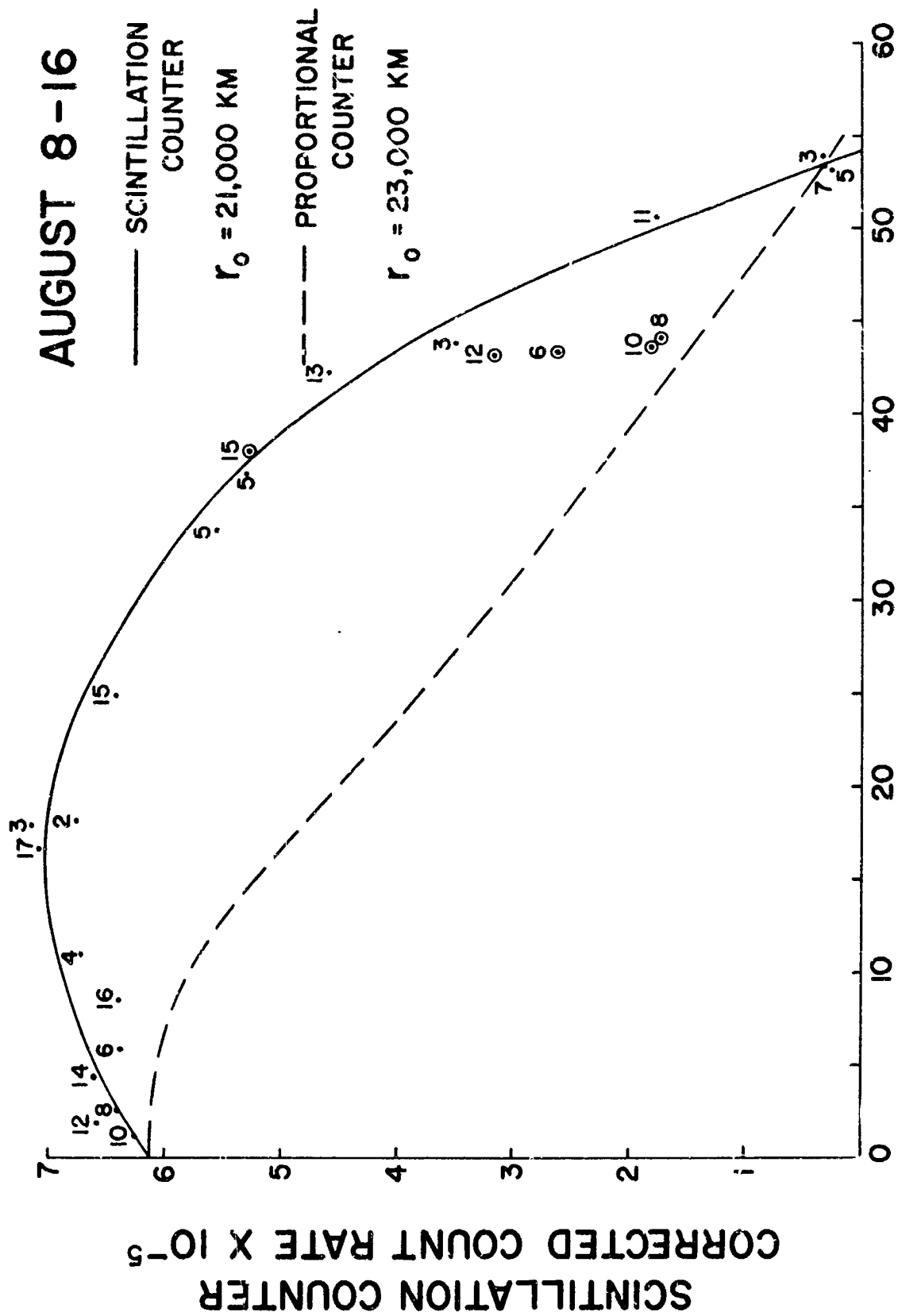
SCINTILLATION COUNTER
CORRECTED COUNT RATE X 10^{-5}

Fig. 3: Radiation detector count rates for the magnetically quiet period from August 8 - 16. The proportional counter rates have been arbitrarily normalized to the scintillation counter-rate at the geomagnetic equator in all count rate figures.
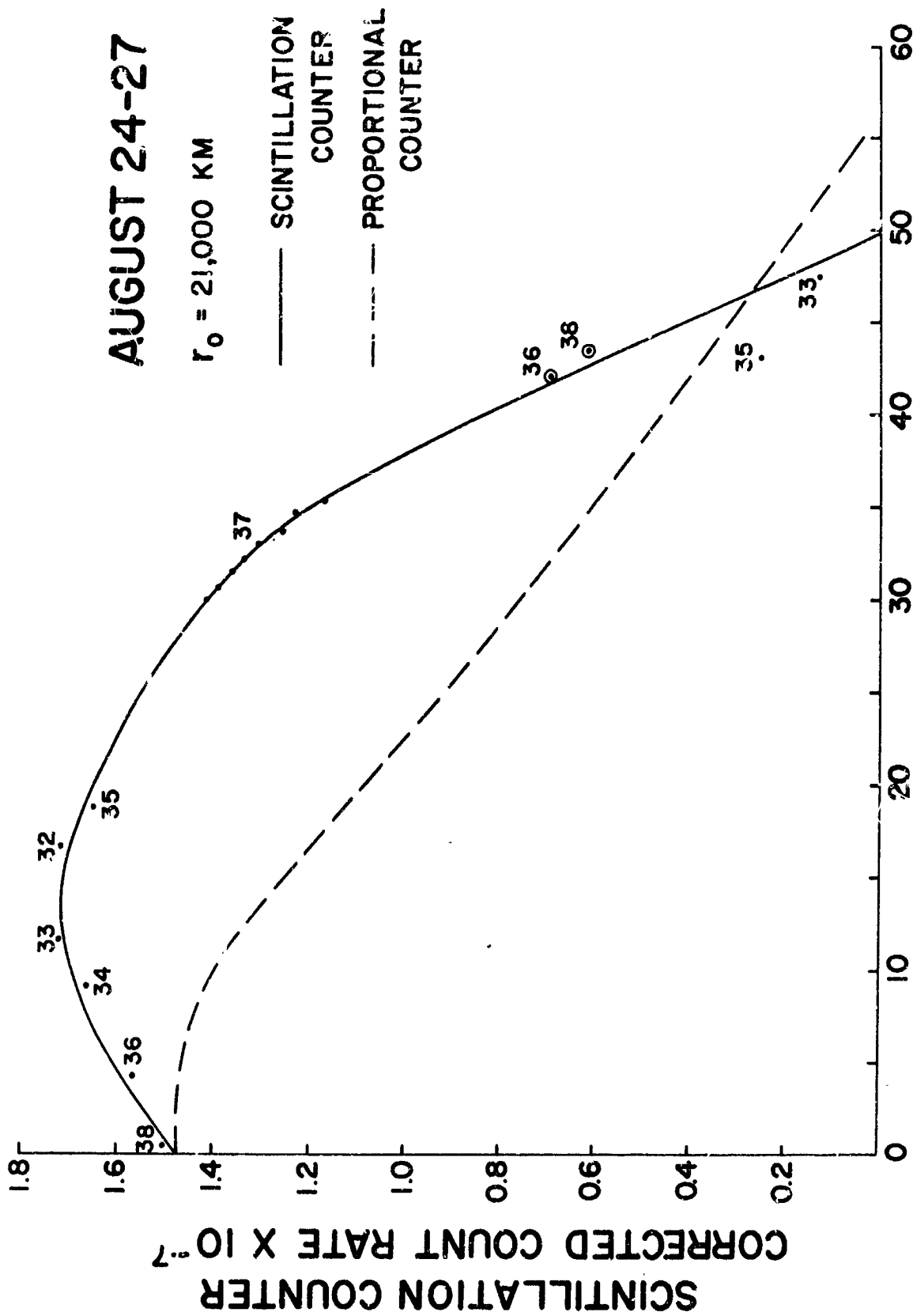
EQUATORIAL PITCH ANGLE DISTRIBUTION

AUGUST 18-22

$r_0 = 21,000$ KM

—— SCINTILLATION COUNTER

- - - PROPORTIONAL COUNTER

$4 \pi \epsilon j \times 10^{-7}$ particles/cm^2 sec ster

3.5   3.0   2.5   2.0   1.5   1.0   0.5

cos α_0

0   0.2   0.4   0.6   0.8   1.0
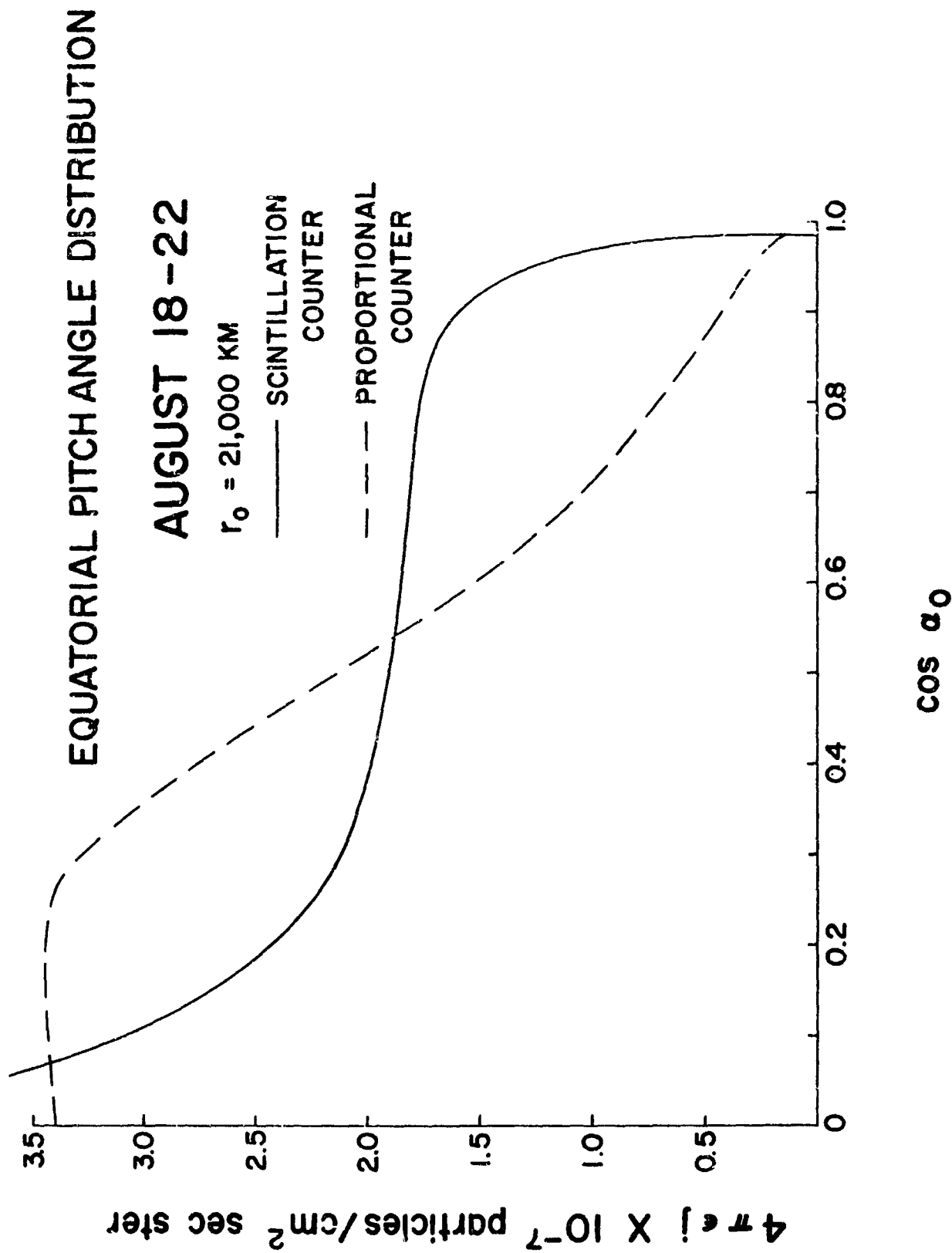
Fig. 4:   Radiation detector count rates for the late recovery phase of the magnetic storm of August 16, 1959.

Fig. 5: Radiation detector count rates for the magnetically quiet period from August 24 - 27.
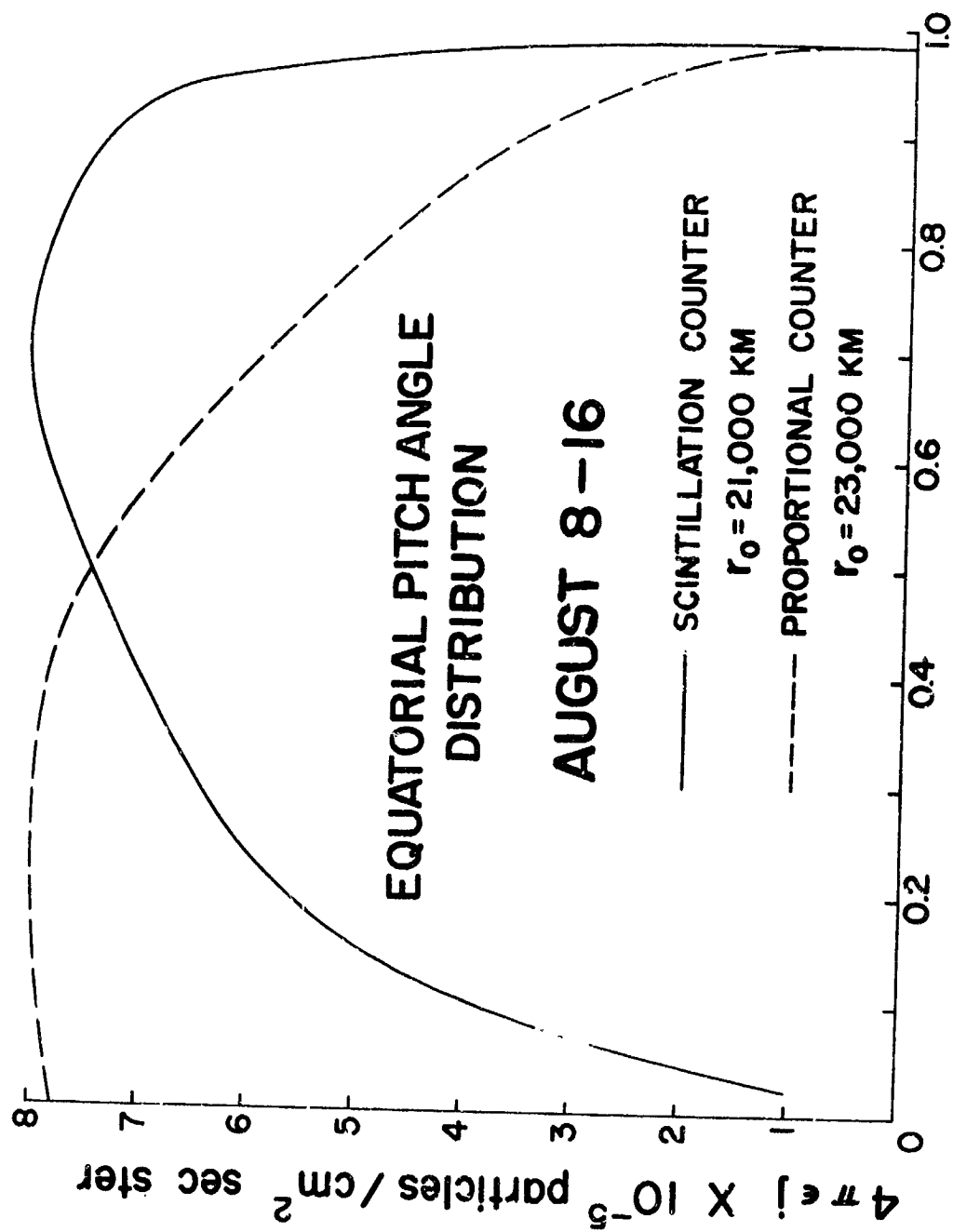
Fig. 6: Pitch angle distributions calculated from the count rates in Fig. 3.
ε is the average efficiency of the detector for the particles to which
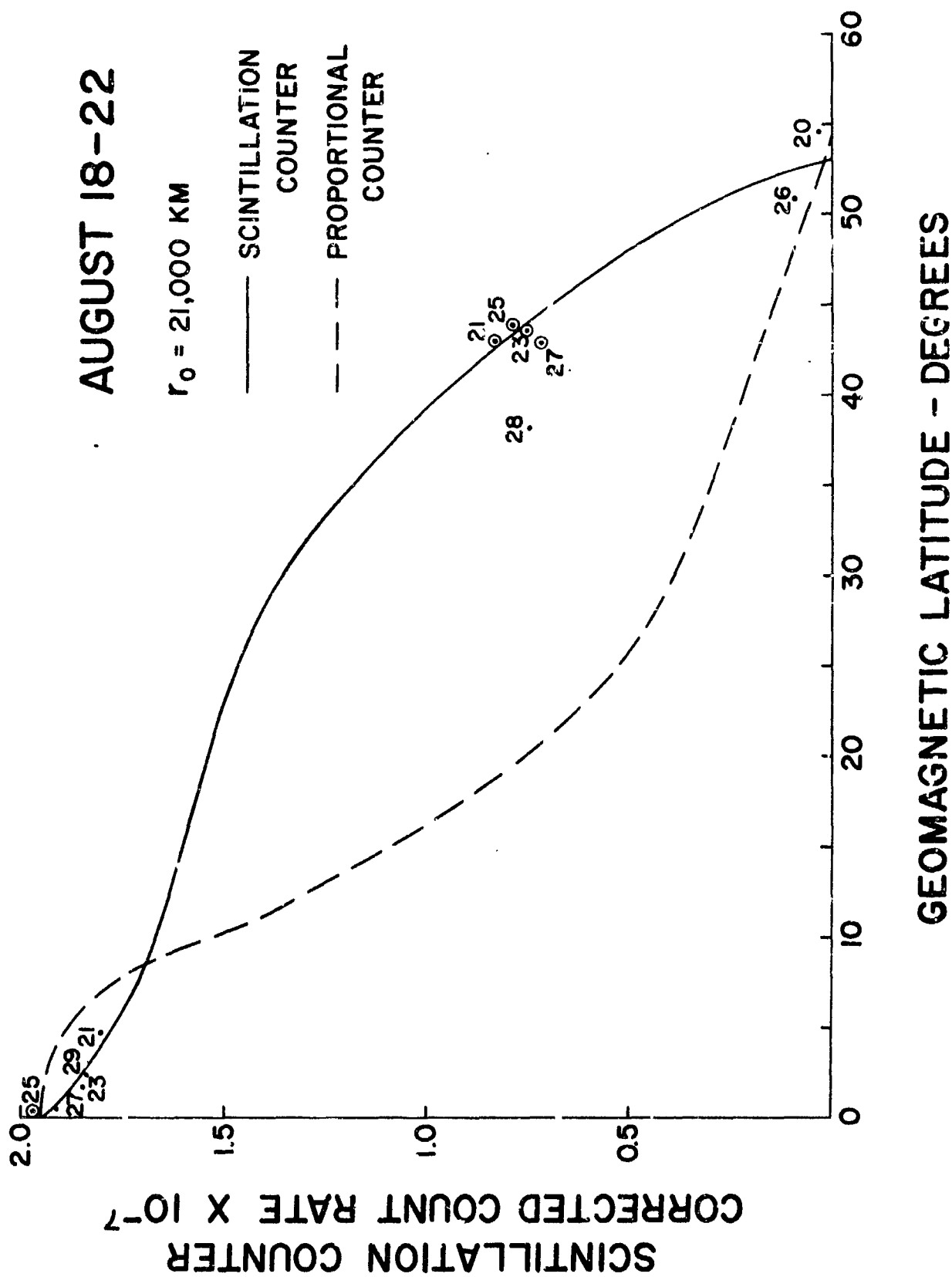the instrument is responding.

Fig. 7:   Pitch angle distributions calculated from the count rates in Fig. 4
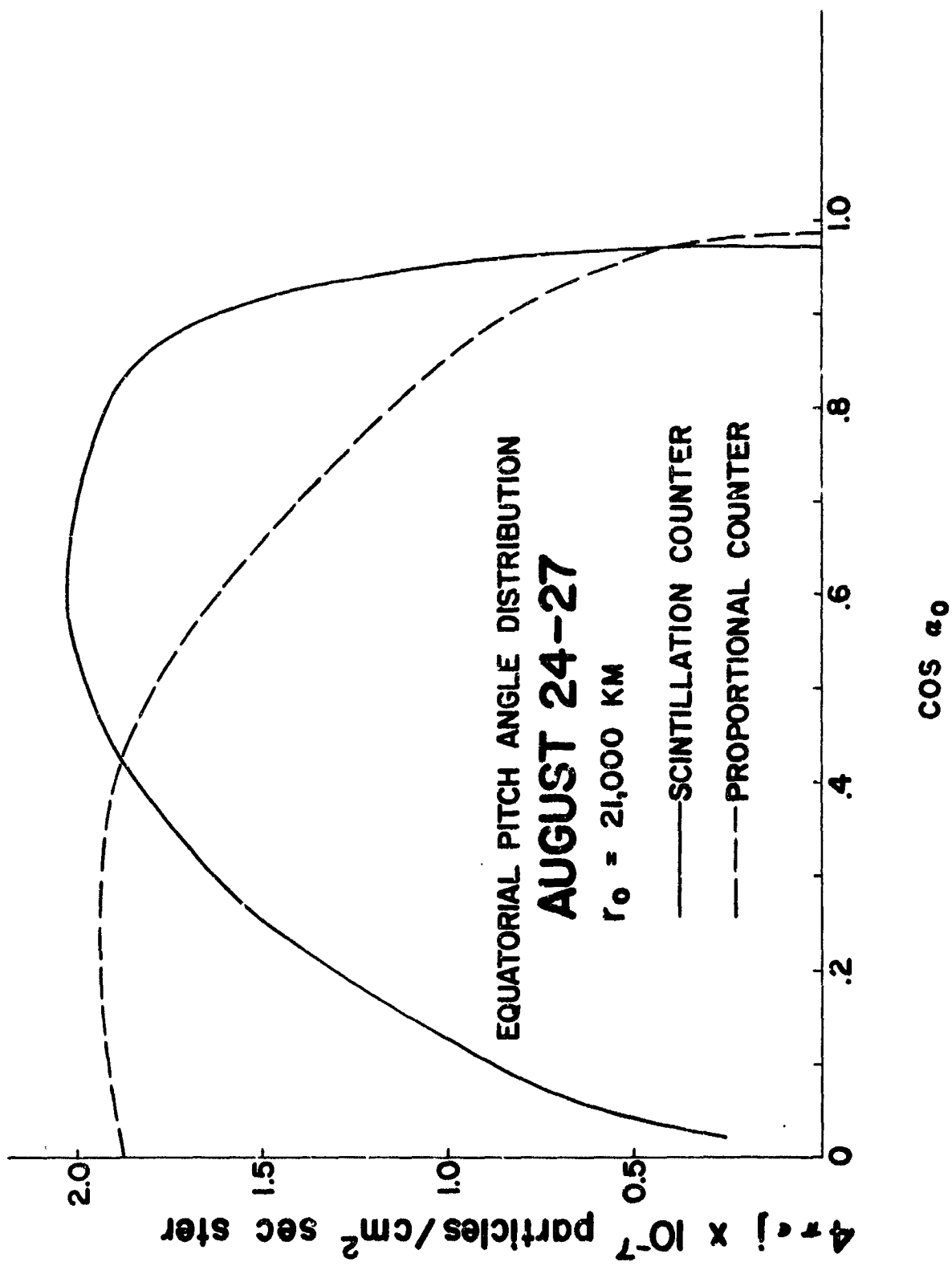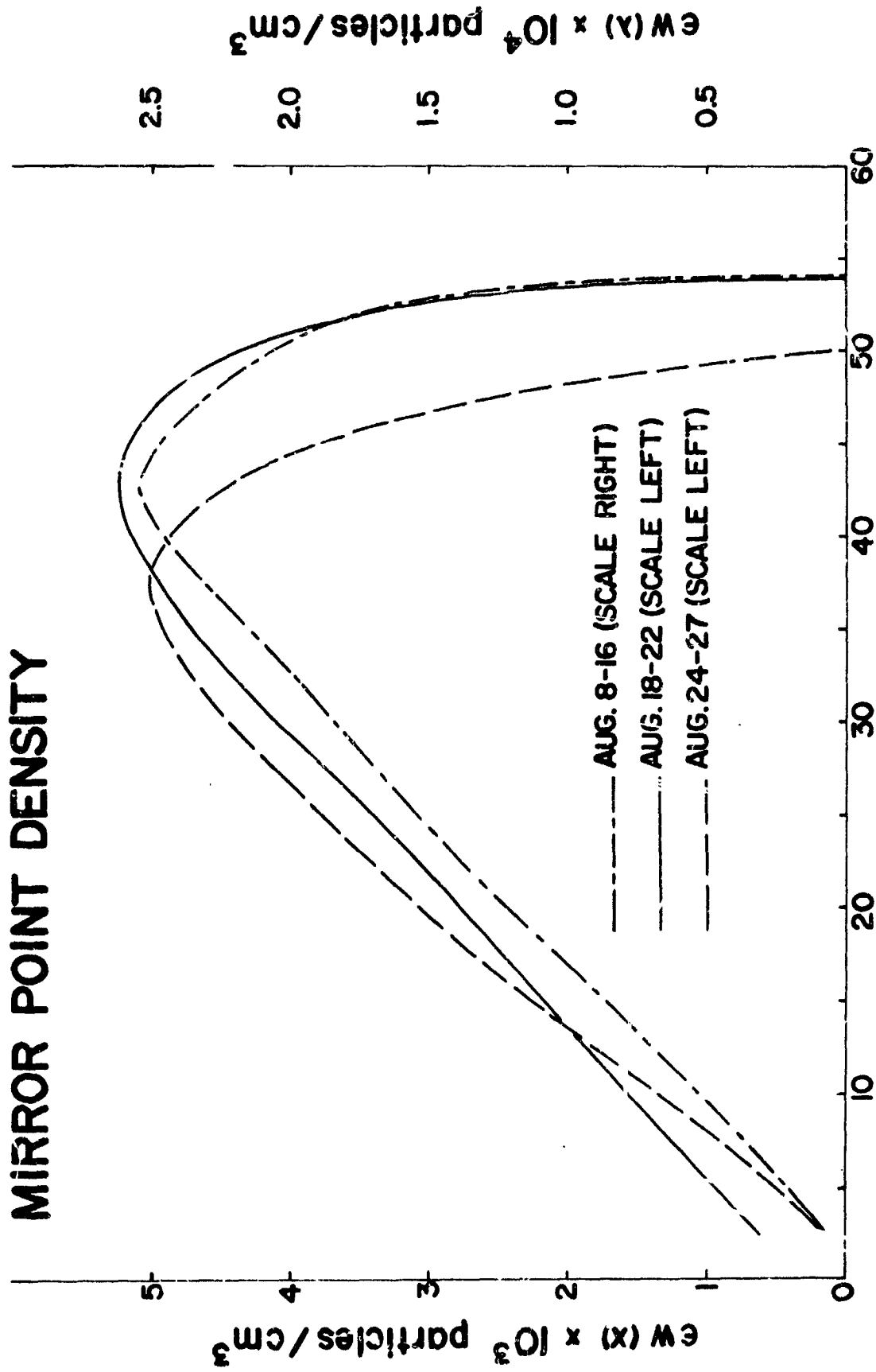
Fig. 8: Pitch angle distributions calculated from the count rates in Fig. 5.

MIRROR POINT DENSITY

GEOMAGNETIC LATITUDE — DEGREES

AUG. 8-16 (SCALE RIGHT)
AUG. 18-22 (SCALE LEFT)
AUG. 24-27 (SCALE LEFT)

Fig. 9: The mirror point density as a function of the latitude at which the particles mirror, using the scintillation counter rates for the three periods considered.

EQUATORIAL PITCH ANGLE DISTRIBUTION

——— AUGUST 8-16
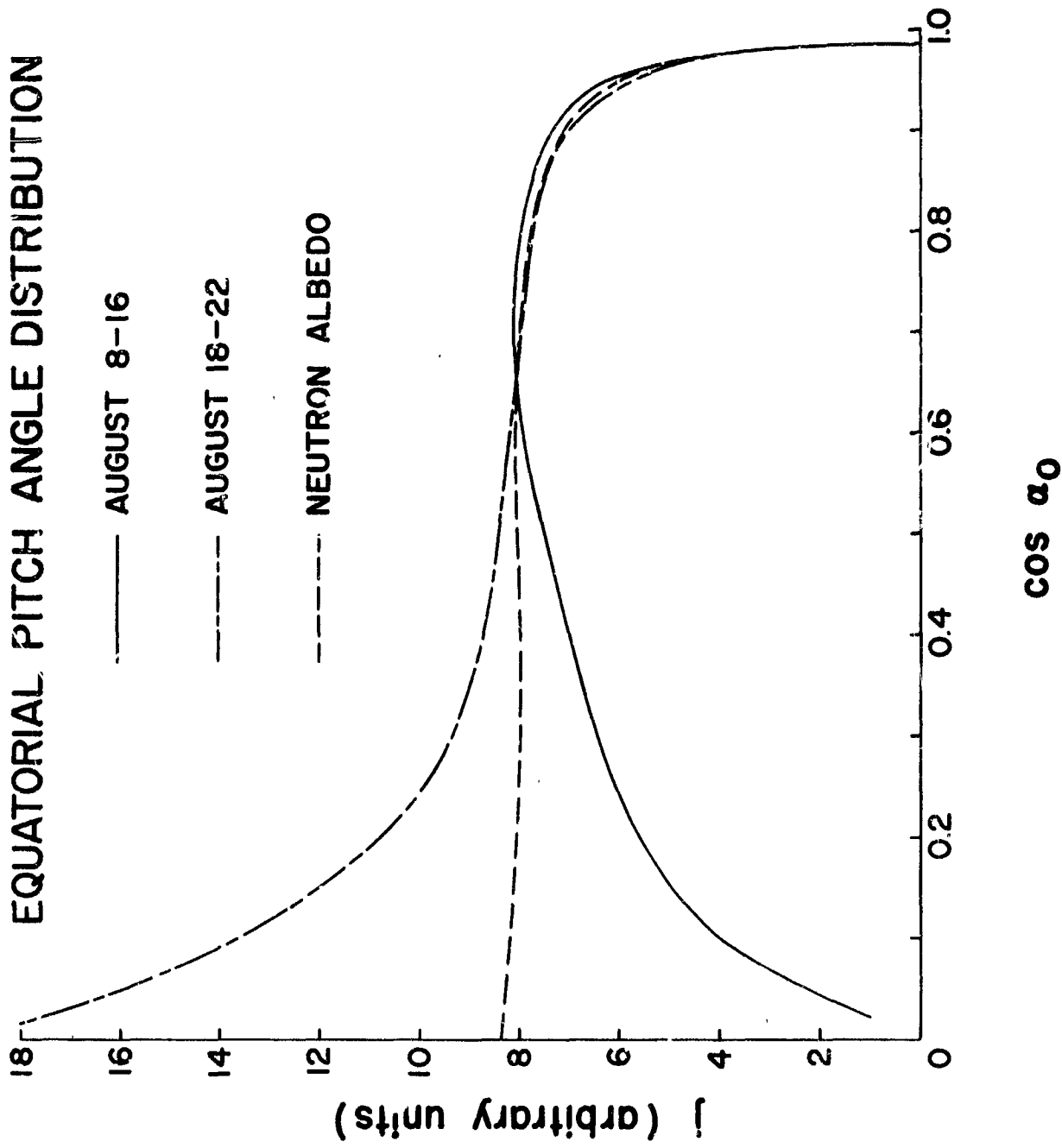
—·—·— AUGUST 18-22

— — — NEUTRON ALBEDO

Fig. 10: Comparison of the August 8 - 16 and August 18 - 22 pitch angle distribution with that calculated from the omnidirectional intensities given by Hess, et al., (1961) for neutron-decay electrons. The curves are arbitrarily normalized at $\cos \alpha_0 = 0.65$.